Physics in Medicine & Biology

IPEM Institute of Physics and Engineering in Medicine

PAPER • OPEN ACCESS

A novel procedure for determining the optimal MLC configuration parameters in treatment planning systems based on measurements with a Farmer chamber

To cite this article: Jordi Saez *et al* 2020 *Phys. Med. Biol.* **65** 155006

IOP Publishing Phys. Med. Biol. 65 (2020) 155006 https://doi.org/10.1088/1361-6560/ab8cd5

Physics in Medicine & Biology

IPEM Institute of Physics and Engineering in Medicine

A novel procedure for determining the optimal MLC configuration parameters in treatment planning systems based on measurements with a Farmer chamber

Jordi Saez[1,5], **Victor Hernandez**[2,5], **Jo Goossens**[3], **Geert De Kerf**[3] and **Dirk Verellen**[3,4]

[1] Department of Radiation Oncology, Hospital Clínic de Barcelona, 08036 Barcelona, Spain
[2] Department of Medical Physics, Hospital Universitari Sant Joan de Reus, IISPV, 43204 Tarragona, Spain
[3] Iridium Kankernetwerk, Antwerp, Belgium
[4] Antwerp University, Faculty of Medicine and Health Sciences, Antwerp, Belgium
[5] The first two authors contributed equally to this work.

E-mail: jordi.saez@gmail.com

Keywords: MLC modelling, TPS modelling, TPS comissioning

Supplementary material for this article is available online

OPEN ACCESS

RECEIVED
31 December 2019

REVISED
8 April 2020

ACCEPTED FOR PUBLICATION
24 April 2020

PUBLISHED
24 July 2020

Abstract

Modelling of the multi-leaf collimator (MLC) in treatment planning systems (TPS) is crucial for the dose calculation accuracy of intensity-modulated radiation therapy plans. However, no standardised methodology for their configuration exists to date. In this study we present a method that separates the effect of each dosimetric characteristic of the MLC, offering comprehensive equations for the determination of the configuration parameters used in the TPS model. The main advantage of the method is that it only requires prior knowledge of the nominal leaf width and is based on doses measured with a Farmer chamber, which is a very well established and robust methodology. Another significant advantage is the required time, since measuring the tests takes only about 30 minutes per energy. Firstly, we provide a theoretical general formalism in terms of the primary fluence constructed from the transmission map obtained from an MLC model for synchronous and asynchronous sweeping beams. Secondly, we apply the formalism to the RayStation TPS as a proof of concept and we derive analytical expressions that allow the determination of the configuration parameters (leaf tip width, tongue-and-groove width, x-position offset and MLC transmission) and describe how they intertwine. Finally, we apply the method to Varian's Millennium120 and HD120 MLCs in a TrueBeam linear accelerator for different energies and determine the optimal configuration parameters. The proposed procedure is much faster and streamlined than the typical trial-and-error methods and increases the accuracy of dose calculation in clinical plans. Additionally, the procedure can be useful for standardising the MLC configuration process and it exposes the limitations of the implemented MLC model, providing guidance for further improvement of these models in TPSs.

1. Introduction

Intensity Modulated Radiation Therapy (IMRT) has been widely adopted as the treatment technique of choice for the majority of photon beam treatments in radiation oncology (Guckenberger *et al* 2017) since it allows for the delivery of complexly shaped dose distributions that help reduce dose to critical structures surrounding target volumes. In order to achieve optimal agreement between planned dose distributions calculated by the treatment planning system (TPS) and measured dose distributions as delivered by the linear accelerator, the configuration of the multi-leaf collimator (MLC) in the TPS constitutes a crucial element. Current MLC designs share two basic mechnanical features: a rounded-leaf end to obtain a consistent penumbra in all leaf positions (Boyer and Li 1997) and a tongue-and-groove (TG) arrangement of adjacent leaves to reduce inter-leaf leakage (Yu 1998). The dosimetric consequences of both characteristics have been extensively studied in the last three decades (LoSasso *et al* 1998, Arnfield *et al* 2000, Chen *et al* 2000, Huq *et al* 2002, Bayouth and Morrill 2003, Vial *et al* 2006, Cadman *et al* 2005, Ling 2003, Thompson *et al* 2014) and it

is well known that the calculation accuracy of TPSs is largely affected by the modelling of these characteristics (Kung and Chen 2000, Williams and Metcalfe 2006, Hardcastle *et al* 2007, Li *et al* 2010).

Commercial TPSs, despite implementing MLC models with diverse levels of sophistication, use similar parameters to describe the main MLC characteristics such as transmission, rounded leaf end and tongue-and-groove effects. Additionally, each TPS manufacturer recommends different procedures to determine the configuration parameters for their MLC model. Some rely on matching beam profiles for a set of static MLC-defined fields (Williams and Metcalfe 2006, Mzenda *et al* 2014, Young *et al* 2016) while others propose a set of test beams for 2D gamma evaluation (Kinsella *et al* 2016, Snyder *et al* 2016). However, due to the limitations of the currently available procedures, a final empiric approach is typically needed. Scientific societies have recognised the need for tuning the MLC parameters, which is consequently recommended in international guidelines (Smilowitz *et al* 2015, Mans *et al* 2016).

Sweeping gap (SG) tests have been commonly used to determine the parameters related to the rounded-leaf end effect, such as the dosimetric leaf gap or leaf offset (LoSasso *et al* 1998, Vial *et al* 2006). Recently, a set of tests named asynchronous sweeping gap (aSG) tests were introduced for the commissioning of the tongue-and-groove effect (Hernandez *et al* 2017). The goals of the present study are: (i) to describe a novel procedure that determines the optimal values of the MLC configuration parameters typically used in TPSs from the measurement results of the SG and aSG tests with a Farmer type ionisation chamber and (ii) to validate that proposed procedure with a set of test beams and clinical cases.

This study focuses on the RayStation TPS, but the method can be easily adapted to other TPSs.

2. Materials and methods

2.1. Sweeping gap tests: general formalism

Let us first briefly re-examine the regular sweeping gap field (SG) in which a given 'sweeping gap' or 'sliding slit' with all leaf pairs perfectly aligned travels a given distance d at constant speed. The actual dose delivered at the centre of the sweeping gap field has two distinct contributions (Kim *et al* 2001, Siebers *et al* 2002): (i) the total primary fluence composed of the direct exposure to the source of primary radiation and the transmission through the MLC leaves and (ii) the scatter of the MLC, which contributes only a small fraction (Kim *et al* 2001) of the total leakage from the MLC and is usually not modelled in commercial TPSs. Consequently, the average dose D_{SG} at the centre of the field can be considered to be proportional to the total primary fluence ϕ_{SG} produced in the area under a leaf pair (Arnfield *et al* 2000), that is,

$$D_{SG} = k\,\phi_{SG}\,, \tag{1}$$

where k is a constant that relates fluence values to dose units. The total primary fluence can be computed from transmission maps following an approach similar to Yu (1998). Thus, because of their symmetry and constant leaf speed, the delivered primary fluence for these tests ϕ_{SG} can be approximated as the integral of the transmission map $T(x, y)$ under a leaf pair with a given width w_{leaf} and across a distance d in the leaf motion direction:

$$\phi_{SG} = \int_0^{w_{leaf}} \int_{-d/2}^{d/2} T(x,y)\,dx\,dy\,. \tag{2}$$

To characterise the sweeping gap beams the *dosimetric leaf separation* or *dosimetric leaf gap* (DLG) is often used. This parameter accounts for the increased transmission through the rounded leaf ends as well as for the MLC calibration and can be modelled by retracting the leaves a certain offset δ equal to half the DLG, which results in an effective gap that can be expressed as:

$$\text{gap}_{\text{eff}} = \text{gap} + \text{DLG} = \text{gap} + 2\,\delta\,. \tag{3}$$

The fluence ϕ_{SG} can be split into two different contributions. The first contribution corresponds to the fluence across open leaves with an effective gap size gap_{eff}. The second contribution is the integrated transmission T across the closed leaf section, which depends on both the distance d travelled by the sweeping gap and the gap size. Hence, for a certain leaf of width w_{leaf}, ϕ_{SG} can be expressed as:

$$\phi_{SG} = w_{leaf}\,\text{gap}_{\text{eff}} + w_{leaf}\,(d - \text{gap}_{\text{eff}})\,T\,. \tag{4}$$

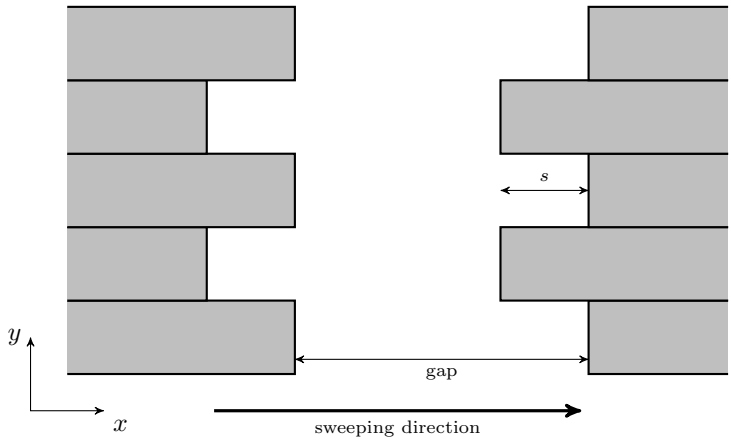

Figure 1. Schematic representation of the asynchronous sweeping gap field in which adjacent leaves are shifted a distance s while keeping the gap constant across the swept field. Jaws are not shown.

Consequently, D_{SG} depends linearly on the effective leaf gap, as described by many authors:

$$D_{SG} = k\,\phi_{SG} = k\,w_{leaf}\left(\text{gap}_{eff}\,(1-T) + d\,T\right)\,. \tag{5}$$

Therefore, D_{SG} also depends linearly on the nominal leaf gap:

$$D_{SG} = \lambda\,\text{gap} + \gamma\,, \tag{6}$$

where

$$\lambda \quad = k\,w_{leaf}\,(1-T)\,, \tag{7a}$$

$$\gamma \quad = k\,w_{leaf}\left(2\delta\,(1-T) + d\,T\right)\,. \tag{7b}$$

These parameters λ and γ can be experimentally obtained and k and δ can be determined as:

$$k \quad = \frac{\lambda}{w_{leaf}\,(1-T)}\,, \tag{8a}$$

$$\delta \quad = \frac{1}{2}\left(\frac{\gamma}{\lambda} - \frac{d\,T}{1-T}\right)\,. \tag{8b}$$

Let us consider next the asynchronous sweeping gap field (aSG) in which adjacent leaves are displaced from each other a certain amount s as illustrated in figure 1, and all leaf pairs move at constant speed while keeping the same nominal gap and MLC shape (Hernandez *et al* 2017). By introducing this shift between adjacent leaves, the tongue and groove regions are exposed, effectively reducing the total primary fluence with respect to the SG test by a certain amount $\Delta\phi_{TG}(s)$ at each side of the leaves:

$$\phi_{aSG}(s) = \phi_{SG} - 2\Delta\phi_{TG}(s)\,. \tag{9}$$

Thus, for the aSG fields:

$$D_{aSG}(s) = k\,(\phi_{SG} - 2\Delta\phi_{TG}) = D_{SG} - 2k\Delta\phi_{TG}(s)\,. \tag{10}$$

For $s = 0$ no tongue-and-groove effect is present and $D_{aSG}(0)$ corresponds identically to the usual sweeping gap test D_{SG}. The fluence reduction caused by the tongue-and-groove can be readily obtained from equation (10) as:

$$\Delta\phi_{TG}(s) = \frac{D_{aSG}(0) - D_{aSG}(s)}{2\,k}\,. \tag{11}$$

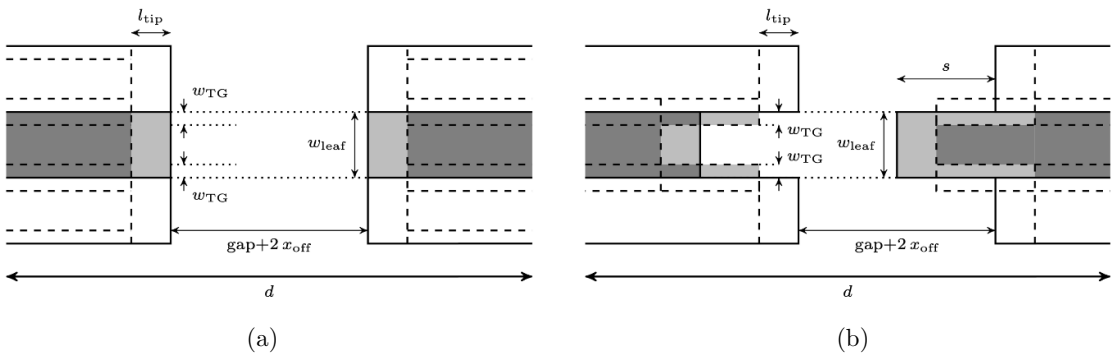

Figure 2. Graphical representation of the MLC model in the RayStation treatment planning system for both (a) sweeping gap and (b) asynchronous sweeping gap fields. Straight lines represent the nominal leaf edges and the fluence is illustrated with dark and light grey shaded areas corresponding to regions with transmission T and $\sqrt{T}$ respectively. Only the regions corresponding to a leaf pair have been shaded.

The previous expression is the generalisation of the function $A(s)$ used previously (Hernandez *et al* 2018) in terms of fluence to facilitate a more comprehensive and general interpretation.

2.2. Description of the RayStation MLC model

The MLC model in the RayStation TPS is characterised by a set of user-definable configuration parameters (RaySearch Labs 2017). A brief description of these parameters is given here:

(a) Transmission T: A single configuration value T for the transmission is used as input for defining the model. Thus, this transmission value should be taken as an average of the interleaf and intraleaf transmissions.
(b) Tongue-and-groove width w_{TG}: The tongue-and-groove region is centered at the leaf side and the width w_{TG} is added both outwards (tongue) and inwards (groove). A transmission value of $\sqrt{T}$ is assigned to this tongue-and-groove region, which has a total width of twice the w_{TG}.
(c) Leaf tip width l_{tip}: The width of a region starting at the leaf tip where a higher transmission value is used to model the increased transmission through the rounded leaf end. In this region a transmission of $\sqrt{T}$ is assigned and neither the tongue nor the groove are modelled.
(d) Position offset: The distance between the DICOM positions of the leaf tip and radiological position used for dose calculations can be adjusted with the parameters MLC x-position offset, gain and curvature. The x-position offset (x_{off}) shifts leaf positions a constant amount regardless of its position, while the parameters gain and curvature allow for the introduction of a second order correction that depends on the leaf position. Thus, at a certain off-axis distance x the position offset can be expressed as (RaySearch Labs 2017):

$$\text{Position offset} = \pm x_{off} + \text{gain} * x \pm \text{curvature} * x^2 , \tag{12}$$

where the $\pm$ sign depends on the MLC bank considered. At the central axis ($x = 0$) the position offset is equal to x_{off}.

2.3. Application to the RayStation MLC model

2.3.1. Sweeping gap tests (SG)

Let us investigate the doses for the sweeping gap tests as calculated by the MLC model described in the previous section. These measurements are typically carried out at the central axis, therefore the gain and curvature parameters can be omitted and the position offset equals x_{off}. The fluence ϕ_{SG} delivered by the SG field tests can be obtained integrating the transmission map for the central leaf (as indicated in Eq 2). This is equivalent to calculating ϕ_{SG} as the sum of the products of the area and the transmission for all the regions under the central leaf as depicted in Fig 2(a):

$$\phi_{SG} = w_{leaf}\left(\text{gap} + 2x_{off} + 2\sqrt{T}l_{tip} + T\left(d - \text{gap} - 2x_{off} - 2l_{tip}\right)\right) . \tag{13}$$

As introduced in equation (4) the dose produced by a sweeping gap without tongue-and-groove is indistinguishable from a simple MLC model that uses an effective leaf gap to account for the increased

transmission through the rounded leaf tip. From equations (4) and (13) it can be deduced that (see details in Supplementary Materials (stacks.iop.org/PMB/65/155006/mmedia)):

$$\mathrm{gap}_{\mathrm{eff}} = \mathrm{gap} + 2x_{\mathrm{off}} + 2\,\frac{\sqrt{T}-T}{1-T}\,l_{\mathrm{tip}}\ , \tag{14}$$

where the last term can be interpreted as twice an offset δ_i introduced by the leaf tip model:

$$\delta_i = \frac{\sqrt{T}-T}{1-T}\,l_{\mathrm{tip}} \tag{15}$$

And the total offset δ, as defined in equation (3), can be related to the configuration parameters in the RayStation MLC model as:

$$\delta = x_{\mathrm{off}} + \delta_i = x_{\mathrm{off}} + \frac{\sqrt{T}-T}{1-T}\,l_{\mathrm{tip}}\ . \tag{16}$$

Hence, the calculated doses for the SG tests are equal to the doses predicted when no leaf tip model is considered and the leaf positions are shifted by a distance $\delta = x_{\mathrm{off}} + \delta_i$. The parameter x_{off} can be understood as an offset due to the MLC positioning calibration (δ_{cal}) and δ_i can be interpreted as an *intrinsic* offset providing the same equivalent fluence as the additional transmission at the leaf tip considered by the MLC model in the TPS.

2.3.2. Asynchronous sweeping gap tests (aSG)

To investigate the fluence reduction caused by the TG effect, the fluence for the aSG fields is evaluated. In this model three different regions can be distinguished depending on the relative amounts of s, l_{tip} and gap^*, defined as $\mathrm{gap}^* = \mathrm{gap} + 2x_{\mathrm{off}}$.

(a) $0 < s \leq l_{\mathrm{tip}}$: since no TG is modelled at the leaf tip, there is no fluence reduction for distances between adjacent leaves smaller than the leaf tip width, hence $\phi_{\mathrm{aSG}}(s) = \phi_{\mathrm{SG}}$ and $\Delta\phi_{\mathrm{TG}}(s) = 0$.

(b) $l_{\mathrm{tip}} < s \leq \mathrm{gap}^* + l_{\mathrm{tip}}$. This situation corresponds to the illustration in figure 2(b). Using equation (2) and accumulating the fluence under the central leaf pair, the fluence can be computed with respect to the $\phi_{\mathrm{SG}}(s)$ given in equation (13) as (see details in Supplementary Materials):

$$\phi_{\mathrm{aSG}}(s) = \phi_{\mathrm{SG}} - 2(s - l_{\mathrm{tip}})\left(1 - 2\sqrt{T} + T\right) w_{\mathrm{TG}}\ . \tag{17}$$

And the fluence reduction results into:

$$\Delta\phi_{\mathrm{TG}}(s) = \frac{\phi_{\mathrm{SG}} - \phi_{\mathrm{aSG}}(s)}{2} = (s - l_{\mathrm{tip}})\left(1 - 2\sqrt{T} + T\right) w_{\mathrm{TG}}\,. \tag{18}$$

This expression shows that in this region the fluence reduction increases linearly with the excess distance over the leaf tip. The slope of the linear relationship is a known function of the transmission T and the width w_{TG}. Note that the fluence reduction caused by the TG effect does not depend on the gap size of the sweeping gap under consideration.

(c) $\mathrm{gap}^* + l_{\mathrm{tip}} < s$. In this region opposing leaves begin to interdigitate and the fluence reduction reaches a maximum that no longer depends on the distance s between neighbouring leaves:

$$\phi_{\mathrm{aSG}}(s) = \phi_{\mathrm{SG}} - 2\,\mathrm{gap}^*\left(1 - 2\sqrt{T} + T\right) w_{\mathrm{TG}}\ .$$

Therefore, the fluence reduction is constant and equal to

$$\Delta\phi_{\mathrm{TG}}(s) = \mathrm{gap}^*\left(1 - 2\sqrt{T} + T\right) w_{\mathrm{TG}}\,.$$

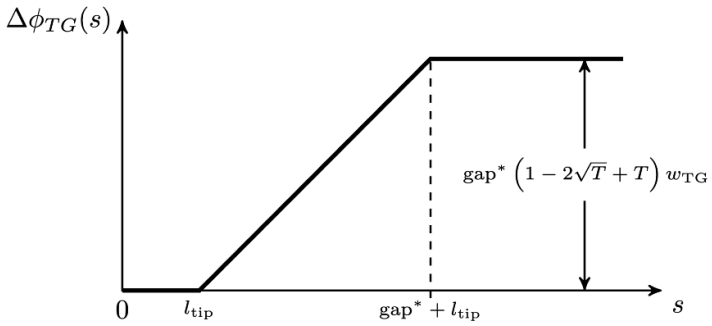

Figure 3. Fluence reduction at a leaf side in RayStation's MLC model.

The calculated fluence reduction for any gap as contiguous leaves are shifted a distance s is represented in figure 3. The curve starts with a flat segment where there is no fluence reduction since the MLC model does not take into account the TG at the leaf tip. As the distance from the leaf tip increases, the fluence reduction increases linearly with a slope that depends on the transmission and the tongue-and-groove width. Finally, a plateau of fluence reduction is reached when leaves interdigitate.

2.4. Procedure for deriving the optimal MLC configuration parameters

In this section the procedure for the determination of the optimal MLC configuration parameters in RayStation is provided. The procedure is based on the measurements of the SG and aSG tests using a Farmer-type ionisation chamber placed at the central axis and the previously derived equations. The length of the Farmer chamber makes it notably suited for these measurements because we want to determine the average doses and this chamber spans several leaves (Hernandez *et al* 2017).

(a) The average transmission T is obtained as the ratio of measurements of a field with all leaves closed and an open field.
(b) A set of measurements of sweeping gaps with different gap sizes is measured to obtain the constant of proportionality between the dose and the nominal gap (λ) and its y-intercept (γ). The constant k that relates fluence to dose can be obtained from λ using equation (8*a*) and the parameter δ can be computed using equation (8*b*).
(c) The asynchronous sweeping gap fields are measured with different distances between neighbouring leaves. The experimental fluence reduction $\Delta\phi_{\text{TG}}^{\text{exp}}(s)$ can be obtained from the sweeping gap doses and the previously obtained constant k (see equation (11)).
(d) The parameters l_{tip} and w_{TG} are obtained by fitting the fluence reduction curve $\Delta\phi_{\text{TG}}$, with the characteristics shown in figure 3, to the experimental fluence reduction $\Delta\phi_{\text{TG}}^{\text{exp}}(s)$.
(e) Finally, the x-offset is computed using equation (16).

In the last step we omitted the gain and curvature because dose calculations at the central axis are independent of these parameters. Gain and curvature can be set to zero as a first approximation, but very small values can be carefully used to fine tune the MLC positions. The gain parameter has no influence on the doses from the sweeping gaps because it shifts the leaf positions in the same direction for both MLC banks and it can be used to compensate for linear discrepancies in the MLC positioning calibration. The curvature parameter directly affects the sweeping gap doses because of the different sign for each MLC bank in equation (12), which for a positive curvature produces a gradual increment in the offset (and in the DLG) at increasing off-axis positions. Thus, the curvature parameter can be assessed in several ways:

(a) From the dose measurement of the SG tests at different off-axis positions. If a different δ value is obtained, this will result in different x_{off} values (see equation (16)) and these differences can be accounted for using equation (12) and an appropriate curvature parameter.
(b) From a measured dose profile along the leaf movement direction (for instance with a detector array or film dosimetry) for a SG beam with a small gap size, e.g. a 2 mm or 5 mm gap. The curvature parameter can then be adjusted to fit the calculated profile to the measured profile.

2.5. Equipment and experiments

The MLC model assessed corresponds to version 9A of the RayStation TPS and the dose calculation algorithm was a collapsed cone convolution. Dose calculations were carried out with both a 1 mm and a 2 mm grid size.

The measurement procedure for determining the optimal configuration parameters was carried out on two TrueBeam linear accelerators (Varian Medical Systems) equipped with a High Definition 120 MLC (HDMLC) and a Millennium120 MLC. Photons with nominal energies of 6 MV with flattening filter (6WFF) and without flattening filter (6FFF), 10 MV (10WFF) and 15 MV (15WFF) with flattening filter.

All measurements were carried out with a Farmer ionisation chamber placed in a water phantom at 10 cm depth and with a source to surface distance of 90 cm.

The following test fields were measured, with jaws set to a 10 cm x 10 cm square field:

(a) Transmission fields for both leaf carriages with leaves closed behind the jaws.
(b) Regular sweeping gap tests for gap sizes 2, 5, 10, 20 and 30 mm. The leaves moved from a position where the gap center was at -60 mm to a position where the gap centre was at +60 mm, travelling a total distance d = 120 mm.
(c) Asynchronous sweeping gap tests for a 20 mm gap size with shifts between adjacent leaves s from 0 to 10 mm in 1 mm steps and from 10 to 30 mm in 2 mm steps.
(d) Asynchronous sweeping gap tests for gaps 5, 10 and 30 mm with several shifts s. These fields were used only to validate that the fluence reduction due to the tongue-and-groove is independent of the leaf gap used and that the same curve $\Delta\phi_{TG}^{exp}(s)$ is obtained regardless of the gap size.

From these measurements the optimal parameters T, l_{tip}, w_{TG} and x_{off} were obtained and compared with a set of initial values obtained following the manufacturer recommended procedure (Savini *et al* 2016), which consisted of profile measurements for a set of static MLC defined fields containing square fields and MLC fields that abutted at the leaf side or with abutting leaf tips.

Finally, the optimal values obtained earlier were validated in a set of clinical plans. In particular, ten stereotactic clinical plans with small target volumes (ranging between 1 and 10 cc) were selected that were considered particularly challenging for the MLC model. The mean MLC gap ranged between 4 and 18 mm and the mean tongue and groove index (Vieillevigne *et al* 2019), defined as the ratio of the tongue and groove length exposed over the corresponding gap, ranged from 0.04 to 0.38. All plans were delivered using a 6FFF energy and the HDMLC onto a solid water plastic phantom (Phantom model 036A from CIRS Inc.) containing an EBT3 radiochromic film placed at the isocentre plane. The films were calibrated in absolute dose and handled according to a well establish protocol (Lewis *et al* 2012). All plans were then calculated with both the initial and optimal set of parameters. A planar dose analysis using the gamma method with a 2 %-2 mm global criteria and a dose threshold set at 10% of the maximum dose was used for comparison.

3. Results

We will develop this section around the results obtained for the HDMLC and the 6MV FFF beam energy. The results and the optimal configuration parameters for other energies and also for the Millennium MLC are reported in table 1. The figures for these other combinations of MLC models and energies are provided as Supplementary Material. The values for the initial parameters obtained from the recommended procedure were $l_{tip} = 3$ mm, $w_{TG} = 0.5$ mm and $x_{off} = 0.2$ mm.

3.1. Measurements and determination of optimal parameters

No differences were found between the 2 mm and 1 mm dose calculation grid sizes. The measured average transmission was 1.03 %, which is in close agreement to values reported in other studies (Kim *et al* 2018).

Results for the SG tests are shown in figure 4(a). A linear regression fit ($r^2 > 0.999\,9$) was carried out on the dose of the SG tests versus the nominal gap, with a proportionality constant $\lambda = 0.614$ Gy/(MU mm) and a y-intercept $\gamma = 1.015$ Gy/MU. Using equation (8*a*) a constant $k = 0.248\,2$ Gy/(MU mm^2) was obtained. The offset δ was calculated from equation (8*b*) as 0.205 mm, which is equivalent to a DLG parameter of 0.41 mm.

The measured doses for the aSG tests for different gap sizes are represented in figure 4(b) as a function of the distance between adjacent leaves s. The figure clearly illustrates the dose reduction caused by the tongue-and-groove effect as leaf sides are increasingly exposed. The experimental fluence reduction $\Delta\phi_{TG}^{exp}(s)$ can be readily computed for all the gap sizes using equation (11) and has been represented in figure 5(a). The curves obtained for different gap sizes coincide for $s <$ gap, demonstrating that the fluence reduction caused by the tongue and groove is independent of the gap size and depends only on the amount of leaf side exposed.

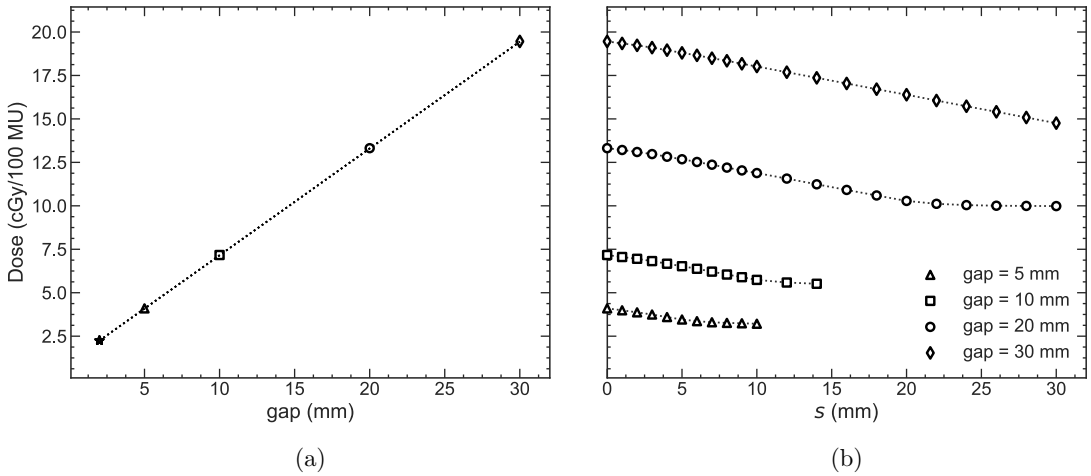

Figure 4. Measured doses for the (a) sweeping gap and (b) asynchronous sweeping gap tests for the 6FFF beam and the HDMLC.

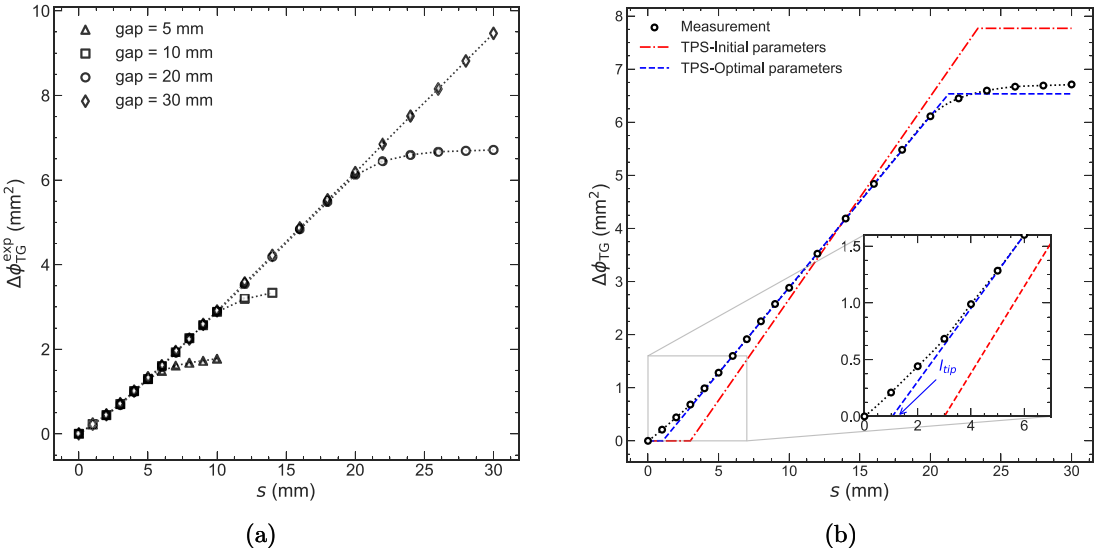

Figure 5. (a) Experimental fluence reduction for the aSG tests obtained for different sweeping gap sizes for the 6FFF beam and the HDMLC. (b) Experimental fluence reduction for the aSG test with a 20 mm gap and the corresponding fit for the MLC model in RayStation.

To derive the optimal configuration parameters we used the $\Delta\phi_{TG}^{exp}(s)$ for the 20 mm gap, depicted in figure 5(b). The experimental fluence reduction exhibits a linear segment for s values between 5 mm and 20 mm. A linear regression fit was carried out in this region and a and slope of 0.322 7 mm was obtained. Using this slope and the transmission value T = 1.03 % the tongue and groove width parameter w_{TG} was computed with equation (18) as w_{TG} = 0.43 mm.

The leaf tip width parameter l_{tip} was also determined through the $\Delta\phi_{TG}^{exp}(s)$ curve. We estimated it as the intersection of the extrapolated linear fit (depicted with a dashed blue line in figure 5(b)) and the abscissa axis, which yielded a value of l_{tip} = 1.05 mm.

The obtained l_{tip} parameter produces an intrinsic offset $\delta_i = 0.107$ mm (see equation (15)). Using equation (16) the offset parameter x_{off} was calculated from δ and δ_i as $x_{off} = 0.12$ mm.

Finally, the curvature was assessed by repeating the sweeping gap test measurements at off-axis positions of -4 cm and +4 cm and recalculating the δ parameter. The values agreed with the δ value measured at the isocentre to within $\pm$ 0.03 mm, which corresponds to differences in the DLG parameter around $\pm$ 0.06 mm. These results indicate that the optimal value for gain and curvature can be considered zero within the experimental uncertainties.

Table 1. Summary of the optimal MLC configuration parameters obtained with the proposed procedure.

	MLCHD		Millennium		
	6 WFF	6 FFF	6 WFF	10 WFF	15 WFFF
T (%)	1.19	1.03	1.46	1.69	1.64
w_{TG} (mm)	0.44	0.43	0.44	0.44	0.44
l_{tip} (mm)	1.19	1.05	1.64	1.81	1.85
x_{off} (mm)	0.12	0.12	0.46	0.50	0.49
DLG (mm)	0.47	0.41	1.28	1.41	1.40
k (Gy/(MU mm^2))	0.262 9	0.248 2	0.132 5	0.147 3	0.154 4

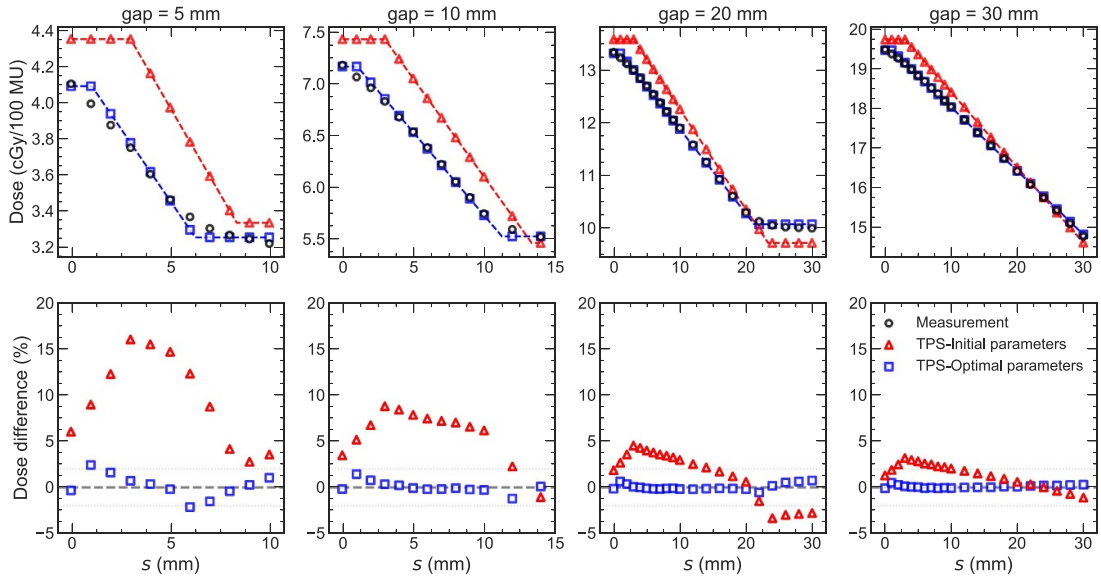

Figure 6. Measured doses and doses calculated with both the initial and the optimal set of parameters for the aSG tests with a 6FFF beam and the HDMLC (upper plots) and dose differences between calculations and measurements (lower plots).

3.2. Validation

The agreement between measured and calculated doses for both the original and the optimal set of configuration parameters was performed in two stages. First the dose agreement for the synchronous and the asynchronous sweeping gaps was evaluated. Then, the agreement in clinical plans was investigated.

3.2.1. Test cases

TPS calculations were carried out for the test fields with both (i) the original set of configuration parameters and (ii) the optimal parameters obtained with the proposed procedure. For each test field the calculated dose was computed as the average dose to a Farmer-type structure in the TPS and compared to the measured dose. Both the calculated and measured doses and the differences between calculations and measurements are represented in figure 6.

The original set of parameters produced dose differences of up to 10 % and 15 % for the smaller sweeping gap tests of 10 mm and 5 mm gap, respectively. When no shift was applied to adjacent leaves ($s = 0$), the doses obtained with the original set of parameters differed only around 2 % from the measured doses except for the smallest sweeping gap of 5 mm, which showed a 5 % difference. However, as adjacent leaves were shifted the dose difference increased and reached a maximum of around $s = 3$ mm. As the distance s increased the dose difference slowly decreased, indicating that the original set of parameter overestimated the dose reduction due to the tongue and groove effect.

On the other hand, the optimal set of parameters provided doses in close agreement with measurements, with differences smaller than 1 % for all gaps except for the 5 mm gap, which yielded a maximum difference of 2 %. The largest discrepancies were found for s values around the leaf tip width parameter (l_{tip} = 1.05 mm) and also when the opposing leaves begin to interdigitate ($s \gtrsim$ gap), coinciding with the regions where the fitted $\Delta\phi_{TG}(s)$ curve differed the most from the experimental curve (see figure 5(b)).

Similar dose differences were obtained for the other combination of MLCs and energies, with the optimal parameters providing an excellent agreement with measured doses.

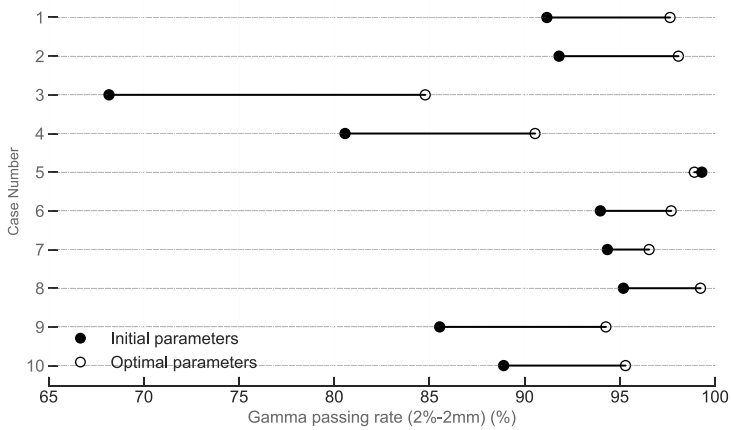

Figure 7. Comparison of gamma analysis results for the selected stereotactic cases with a 2–2 mm criteria for both the original set of MLC configuration parameters and the optimal set of parameters derived with procedure described in the text.

3.2.2. Clinical cases

When the MLC configuration parameters in table 1 for the 6FFF beam and the MLCHD were used in the clinical plans the gamma passing rate improved significantly with respect to the passing rates obtained with the initial configuration parameters (see figure 7).

4. Discussion

We have described a novel procedure for the determination of the MLC configuration parameters based on synchronous and asynchronous sweeping gaps and measurements with a Farmer chamber. This chamber is recommended because the method is based on average doses and consequently a sufficient length to integrate the doses from different parts of several leaves is needed. Alternatively, a semiflex ion chamber could be used, but the Farmer chamber is preferred due to its greater length and active volume. The major advantage of this procedure is that it separates the effect of each dosimetric characteristic of the MLC, offering comprehensive equations for the determination of the configuration parameters used in the TPS model. Additionally, the derived equations clearly illustrate the intricate relationships between the different configuration parameters and how they intertwine. Furthermore, the method only requires prior knowledge of the nominal leaf width and is based on doses measured with a Farmer chamber, which is a very well established and robust methodology (LoSasso *et al* 1998, Arnfield *et al* 2000). Another significant advantage is the required time, since measuring the tests takes only about 30 minutes per energy as opposed to the time-consuming process of iteratively tuning the parameters for optimising the dose agreement for clinical plans.

We found that a tongue and groove width of 0.44 mm is suitable for both the MLCHD and the Milllennium regardless of the beam energy. This result is consistent with the fact that both MLCs share the same tongue and groove design and physical width. Values of around 0.33 mm have been reported for the same MLC models and another TPS (Hernandez *et al* 2017), but this is compatible with the values obtained in the present study because the 0.33 mm value was obtained for an MLC model that assigned null transmission to this region. Interestingly, the corresponding fluence reduction is indistinguishable from the reduction in which zero transmission is assigned to the tongue and groove width provided that the dose calculation grid is larger than the tongue and groove width. Despite that, an MLC model that considers both the tongue and the groove widths can better model the regions of overlap between the tongue and the groove of adjacent leaves and provide more accurate dose calculations.

Regarding the leaf tip width, the value obtained for the MLCHD (~ 1.1 mm) is smaller than the value obtained for the Millennium MLC (~ 1.7 mm). This was expected because the radius of the rounded leaf end for the HDMLC is double that of the Millennium leaves (16 cm and 8 cm, respectively). The leaf tip width exhibits a modest energy dependence, with slightly larger values for higher energies.

We showed that the total offset can be divided into two different components. The first is the intrinsic offset, which is a direct consequence of the leaf tip model and the increased transmission across the rounded leaf end. The second is the offset due to the leaf positioning calibration. Our results show that the total offset δ (equal to half the dosimetric leaf gap) is energy dependent. On the other hand, when the intrinsic offset is removed the remaining x-offset is rather constant for the different energies, which supports this interpretation of intrinsic and calibration offsets.

Finally, the gain and curvature should be set to zero as a first approximation. These parameters can be used to account for a second order correction in the leaf positions at off-axis distances, but their use should be carefully evaluated. For instance, some investigators have reported slight variations in the DLG at off-axis positions (Kumaraswamy *et al* 2014, Mei *et al* 2011). The curvature parameter can be used to model these variations, but we recommend that a thorough validation is carried out in those cases.

Our approach explicitly highlights the fact that the MLC configuration parameters intertwine in complex ways. As a consequence, when these parameters are determined by tentatively trying to maximise the agreement between calculations and measurements for clinical plans some compensations might take place, producing a reasonably good modelling for a particular set of treatment plans but not for other plans with different characteristics. This could explain why the need to configure various MLC models for plans with different characteristics (Kielar *et al* 2012, Yao and Farr 2015, Kim *et al* 2018) has been reported. An example of such entanglement was recently shown for the Eclipse TPS, in which tuning of the dosimetric leaf gap in the TPS could compensate for limitations in their tongue and groove model (Vieillevigne *et al* 2019).

Another important advantage of our procedure is that it reveals the limitations of the MLC model implemented in the TPS, identifying the main aspects in need of improvement. For instance, for both MLCs considered in the present study, the largest differences between the calculated and the experimental fluence reductions take place for 's' values in the first few millimetres because the current MLC model does not account for the tongue and groove at the leaf tip. A possible development to overcome this limitation might be to assign a variable tongue width or a variable transmission in the tongue and groove regions (Hernandez *et al* 2018). A simpler and more straightforward improvement would be to assign, as a first approximation, a certain constant transmission to the tongue and groove region at the leaf tip such as $T^{1/4}$ (i.e. the square of the transmission assigned to the leaf tip width). This transmission would produce a certain slope in the calculated $\Delta\phi$ at the region $0 < s < l_{\text{tip}}$, improving the agreement between calculated and measured doses in the first few millimetres (< 5 mm). Note that a larger tip width would then be required to reach the intersection with the linear region of $\Delta\phi^{\text{exp}}$. Hence, the intrinsic offset δ_i would be larger and the x-offset parameter should be decreased to keep the total offset (and the doses for the SG beams) unaltered.

In a recent analysis (Kerns *et al* 2017) of the IROC-Houston anthropomorphic phantom irradiations, submitted plans were recalculated using an independent calculation system that used generic reference beam data. For a vast majority of the participating centers (68%) that failed the credentialing process, recalculations with the reference beam data had greater accuracy than the institution's TPS, which suggests a poor modelling of the TPS. The same group has recently published the reference dataset of users' photon beam modelling parameters gathered through an electronic survey with a questionnaire (Glenn *et al* 2019). Parameters were collected from 642 institutions for Eclipse, Pinnacle and RayStation and a large variability was found in the MLC configuration parameters. This large variability could be the reason behind the results found by Kerns *et al.* We believe that these variations are mainly due to the lack of standardised procedures and to the different methodologies used in the determination of these parameters rather than to real differences in the MLC characteristics and that the systematic and comprehensive methodology and tests described in this study could be adapted to other TPSs. The rationale is that each TPS has a certain calculated $\Delta\phi_{\text{TG}}(s)$ curve that depends on its MLC configuration parameters and fitting this curve to the experimental $\Delta\phi_{\text{TG}}^{\text{exp}}(s)$ curve will therefore allow the determination of these parameters. For instance, the 'tongue and groove width' parameter in Pinnacle (Williams and Metcalfe 2006) and the 'leaf groove width' parameter in Monaco (Kinsella *et al* 2016) could also be determined from the slope in the linear region of the experimental $\Delta\phi_{\text{TG}}^{\text{exp}}(s)$. Depending on the leaf tip model of each TPS a different expression for the intrinsic offset δ_i will be obtained and the parameters related to the leaf tip model ('rounded leaf tip radius' and 'leaf offset calibration' in Pinnacle, 'leaf tip leakage' and 'leaf tip offset' in Monaco) could also be derived similarly to x-offset and l_{tip} in RayStation. As a consequence, the proposed methodology can be helpful for standardising the configuration of MLC models in TPSs and for reducing the variability in the parameters used in different centres.

A limitation of the present study is that the expressions derived are specific to a particular TPS. However, the procedure could be applied in general to other TPSs as long as the effect of each configuration parameter is known and the total primary fluence for the sweeping gaps can be computed. Another limitation is that only Varian MLC models were evaluated, although the method is valid for any MLC. Future work will address other MLC models, as well as the variability of the MLC configuration parameters obtained with this procedure in different institutions.

5. Conclusions

We have presented a comprehensive and robust procedure for obtaining the optimal value for the configuration parameters of an MLC model based on measurements with a Farmer chamber for a set of

modified sweeping gap tests[1]. The proposed procedure is much faster and streamlined than the typical trial-and-error methods and increases the dose calculation accuracy in clinical plans. Additionally, the procedure can be useful for standardising the MLC configuration process and it reveals the limitations of MLC models, providing guidance for their further improvement in TPSs.

Acknowledgments

The authors would like to thank Agnes Angerud, from RaySearch Labs, for clarifying some of the details of the MLC model in the studied version of the RayStation TPS and for her critical review of the manuscript. We would also like to thank Eduardo Fuentes at BioTerra, S.L. for kindly providing access to a RayStation test server during the preliminary part of this study.

Disclosure of conflicts of interest

Some of the authors (JG, GDK, DV) have a research agreement with RaySearch Labs.

ORCID iDs

Jordi Saez https://orcid.org/0000-0003-4888-9323
Victor Hernandez https://orcid.org/0000-0003-3770-8486
Jo Goossens https://orcid.org/0000-0002-2149-6987
Geert De Kerf https://orcid.org/0000-0002-3314-0128
Dirk Verellen https://orcid.org/0000-0002-0734-6464

References

Arnfield M R, Siebers J V, Kim J O, Wu Q, Keall P J and Mohan R 2000 A method for determining multileaf collimator transmission and scatter for dynamic intensity modulated radiotherapy *Med. Phys.* **27** 2231–41
Bayouth J E and Morrill S M 2003 Mlc dosimetric characteristics for small field and imrt applications *Med. Phys.* **30** 2545–52
Boyer A L and Li S 1997 Geometric analysis of light-field position of a multileaf collimator with curved ends *Med. Phys.* **24** 757–62
Cadman P, McNutt T and Bzdusek K 2005 Validation of physics improvements for imrt with a commercial treatment-planning system *J. Appl. Clin. Med. Phys.* **6** 74–86
Chen Y, Boyer A L and Ma C-M 2000 Calculation of x-ray transmission through a multileaf collimator *Med. Phys.* **27** 1717–26
Glenn M C, Peterson C B, Followill D S, Howell R M, Pollard-Larkin J M and Kry S F 2019 Reference dataset of users' photon beam modeling parameters for the eclipse, pinnacle and raystation treatment planning systems *Med. Phys.* **47** 282–88
Guckenberger M *et al* 2017 Estro acrop consensus guideline on implementation and practice of stereotactic body radiotherapy for peripherally located early stage non-small cell lung cancer *Radiother. Oncol.* **124** 11–17
Hardcastle N, Metcalfe P, Ceylan A and Williams M J 2007 Multileaf collimator end leaf leakage: implications for wide-field imrt *Phys. Med. Biol.* **52** N493–N504
Hernandez V, Vera-Sánchez J A, Vieillevigne L, Khamphan C and Saez J 2018 A new method for modelling the tongue-and-groove in treatment planning systems *Phys. Med. Biol.* **63** 245005
Hernandez V, Vera-Sánchez J A, Vieillevigne L and Saez J 2017 Commissioning of the tongue-and-groove modelling in treatment planning systems: from static fields to vmat treatments *Phys. Med. Biol.* **62** 6688–707
Huq M S, Das I J, Steinberg T and Galvin J M 2002 A dosimetric comparison of various multileaf collimators *Phys. Med. Biol.* **47** N159–N170
Kerns J R, Stingo F, Followill D S, Howell R M, Melancon A and Kry S F 2017 Treatment planning system calculation errors are present in most imaging and radiation oncology core-houston phantom failures *Int. Journal of Radiation Oncology* Biology* Physics* **98** 1197–203
Kielar K N, Mok E, Hsu A, Wang L and Luxton G 2012 Verification of dosimetric accuracy on the truebeam stx: Rounded leaf effect of the high definition mlc *Med. Phys.* **39** 6360–71
Kim J, Han J S, Hsia A T, Li S, Xu Z and Ryu S 2018 Relationship between dosimetric leaf gap and dose calculation errors for high definition multi-leaf collimators in radiotherapy *Phys Imag Radiat Oncol* **5** 31–6
Kim J O, Siebers J V, Keall P J, Arnfield M R and Mohan R 2001 A monte carlo study of radiation transport through multileaf collimators *Med. Phys.* **28** 2497–506
Kinsella P, Shields L, McCavana P, McClean B and Langan B 2016 Determination of mlc model parameters for monaco using commercial diode arrays *J. Appl. Clin. Med. Phys.* **17** 37–47
Kumaraswamy L K, Schmitt J D, Bailey D W, Xu Z Z and Podgorsak M B 2014 Spatial variation of dosimetric leaf gap and its impact on dose delivery *Med. Phys.* **41** 111711
Kung J H and Chen G T Y 2000 Intensity modulated radiotherapy dose delivery error from radiation field offset inaccuracy *Med. Phys.* **27** 1617–22
Lewis D, Micke A, Yu X and Chan M F 2012 An efficient protocol for radiochromic film dosimetry combining calibration and measurement in a single scan *Med. Phys.* **39** 6339–50
Li J S, Lin T, Chen L, Price R A and Ma C-M 2010 Uncertainties in imrt dosimetry *Med. Phys.* **37** 2491–500
(Ling) M S-K C C 2003 *A Practical Guide to Intensity-Modulated Radiation Therapy* Medical Physics Publishing

[1]The DICOM files for the tests will be provided by the authors upon request.

LoSasso T, Chui C-S and Ling C C 1998 Physical and dosimetric aspects of a multileaf collimation system used in the dynamic mode for implementing intensity modulated radiotherapy *Med. Phys.* **25** 1919–27

Mans A *et al* 2016 The ncs code of practice for the quality assurance and control for volumetric modulated arc therapy *Phys. Med. Biol.* **61** 7221–35

Mei X, Nygren I and Villarreal-Barajas J E 2011 On the use of the mlc dosimetric leaf gap as a quality control tool for accurate dynamic imrt delivery *Med. Phys.* **38** 2246–55

Mzenda B, Mugabe K V, Sims R, Godwin G and Loria D 2014 Modeling and dosimetric performance evaluation of the raystation treatment planning system *J. Appl. Clin. Med. Phys.* **15** 29–46

RaySearch Labs 2017 *Raystation 6 - Reference Manual* RaySearch Labs

Savini A, Bartolucci F, Fidanza C, Rosica F and Orlandi G 2016 Po-0806: Optimisation and assessment of the mlc model in the raystation treatment planning system *Radiother. Oncol.* **119** S380–S381

Siebers J V, Keall P J, Kim J O and Mohan R 2002 A method for photon beam monte carlo multileaf collimator particle transport *Phys. Med. Biol.* **47** 3225–49

Smilowitz J B *et al* 2015 AAPM Medical Physics Practice Guideline 5.a.: Commissioning and QA of Treatment Planning Dose Calculations - Megavoltage Photon and Electron Beams *J. Appl. Clin. Med. Phys.* **16** 14–34

Snyder M, Halford R, Knill C, Adams J N, Bossenberger T, Nalichowski A, Hammoud A and Burmeister J 2016 Modeling the agility mlc in the monaco treatment planning system *J. Appl. Clin. Med. Phys.* **17** 190–202

Thompson C M, Weston S J, Cosgrove V C and Thwaites D I 2014 A dosimetric characterization of a novel linear accelerator collimator *Med. Phys.* **41** 031713

Vial P, Oliver L, Greer P B and Baldock C 2006 An experimental investigation into the radiation field offset of a dynamic multileaf collimator *Phys. Med. Biol.* **51** 5517–38

Vieillevigne L, Khamphan C, Saez J and Hernandez V 2019 On the need for tuning the dosimetric leaf gap for stereotactic treatment plans in the eclipse treatment planning system *J. Appl. Clin. Med. Phys.* **20** 68–77

Williams M J and Metcalfe P 2006 Verification of a rounded leaf-end mlc model used in a radiotherapy treatment planning system *Phys. Med. Biol.* **51** N65–N78

Yao W and Farr J B 2015 Determining the optimal dosimetric leaf gap setting for rounded leaf-end multileaf collimator systems by simple test fields *J. Appl. Clin. Med. Phys.* **16** 65–77

Young L A, Yang F, Cao N and Meyer J 2016 Rounded leaf end modeling in pinnacle vmat treatment planning for fixed jaw linacs *J. Appl. Clin. Med. Phys.* **17** 149–62

Yu C X 1998 Design considerations for the sides of multileaf collimator leaves *Phys. Med. Biol.* **43** 1335–42